Dynamic and Conventional Spin-Echo MR of Pituitary Microlesions

Walter S. Bartynski and Luke Lin

PURPOSE: To determine whether dynamic traditional spin-echo MR imaging, with the use of routine T1 parameters during contrast infusion, is superior to standard MR imaging after contrast administration for detecting microlesions of the pituitary gland. **METHODS:** Sixty-four patients with pituitary microlesions 3 to 10 mm in diameter were examined with a dynamic traditional spin-echo technique; that is, a typical T1 spin-echo sequence of 500–600/20–25/2 (repetition time/echo time/excitations), 3-mm-thick sections, 16-cm field of view, 256 × 128 matrix, and a scan time ranging from 2 minutes to 2 minutes 40 seconds during contrast infusion. In addition, standard imaging with unenhanced and contrast-enhanced spin-echo sequences were obtained. The three sequences were evaluated retrospectively and graded for gland-lesion contrast conspicuity, lesion homogeneity, and delineation of lesion margin. **RESULTS:** The dynamic sequence was judged to be better than the standard enhanced sequence for depicting microlesions in 42% to 47% of patients. Lesions were identified only on the dynamic study in an additional 11% to 14% of patients. Lesions were seen equally well on the standard and dynamic sequences only in 16% to 23% of cases. The standard postcontrast sequence was judged better in 12.5% to 17% of cases, with lesions identified only on the standard sequence in an additional 8% to 9%. **CONCLUSION:** Dynamic traditional spin-echo MR imaging improved lesion detection and provided increased clarity over standard sequences after contrast infusion. Both sequences are important, since lesions were detected only on the dynamic sequence in 11% to 14% of patients and only on the standard sequence in 8% to 9% of patients.

Index terms: Pituitary gland, magnetic resonance; Magnetic resonance, technique

AJNR Am J Neuroradiol 18:965–972, May 1997

In the early 1980s, Hemminghytt et al (1) noted that detection of pituitary microadenoma with computed tomography (CT) was time dependent after contrast administration. This was postulated to be due to a difference in the time course of enhancement of the microadenoma relative to the adjacent normal gland. Bonneville et al (2) described the CT pattern of pituitary enhancement early after contrast infusion, and encouraged the use of dynamic scanning in the evaluation of microadenomas.

A similar time dependence in gland enhancement and adenoma-gland contrast difference has been documented with magnetic resonance (MR) imaging (3–7). MR imaging studies have generally been obtained with either signal-limited rapid T1 techniques or unique sequences not available on most MR imaging systems. The purpose of our investigation was to determine whether dynamic traditional spin-echo imaging, with the use of a traditional spin-echo technique but during contrast infusion, resulted in improved lesion detection relative to routine imaging after contrast administration.

Materials and Methods

Four hundred forty-four MR imaging examinations of the pituitary gland were performed at our institution during a 7-year period. In 187 studies, a macroadenoma was present, prior surgery had been performed, or a pituitary lesion previously studied by MR imaging was present. These cases were excluded from the study. Two hundred fifty-seven examinations were therefore available in which the gland was of normal size and there was no previously known lesion. In 64 (25%) of these 257 patients, a new microadenoma or microlesion was identified in the pitu-

Received June 13, 1996; accepted after revision November 22.

From the Department of Radiology, Western Pennsylvania Hospital, 4800 Friendship Ave, Pittsburgh, PA 15224. Address reprint requests to W. S. Bartynski, MD.

AJNR 18:965–972, May 1997 0195-6108/97/1805–0965

TABLE 1: Dynamic and conventional pituitary imaging protocol

Type of Sequence	Section Thickness, mm	Repetition Time, ms	Echo Time, ms	No. of Excitations	Matrix Size	Field of View, cm	Time, min
Sagittal scout	3	300	20	1	256 × 128	24	0:47
Coronal unenhanced	3	500–600	20–25	2	256 × 192	16	3:50
Coronal dynamic contrast enhanced*	3	500–600	20–25	2	256 × 128	16	2:41
Coronal standard contrast enhanced	3	500–600	20–25	4	256 × 128	16	5:10

* This sequence included prescanning, insertion of intravenous tubing, repositioning of patient, injection of one third contrast bolus, and scanning during injection of remaining two thirds of contrast bolus.

itary gland. These 64 lesions form the basis of this report. All studies were obtained on a 1.5-T MR imaging unit. Examinations were performed with a dynamic traditional spin-echo enhancement technique acquired during contrast infusion in addition to a standard postcontrast technique.

Dynamic Traditional Spin-Echo Technique

The dynamic traditional spin-echo technique is a routine spin-echo sequence obtained during contrast infusion. Imaging sequences and parameters are reviewed in Table 1. A sagittal scout view (300/20/1 [repetition time/echo time/excitation], 3-mm-thick sections, 24-cm field of view [FOV], 256 × 128 matrix, 47-second scan time) was obtained, followed by a routine unenhanced coronal T1-weighted sequence of the pituitary gland (500–600/20–25/2, 3-mm-thick sections, 16-cm FOV, 256 × 192 matrix, 3-minute 50-second scan time).

Manual or automatic prescanning was then performed to tune the MR imaging system before contrast infusion and before beginning data acquisition for the dynamic spin-echo sequence. When the prescan was completed, the patient was removed from the magnet bore and a butterfly needle was inserted into an antecubital vein. The contrast syringe, with extension tubing, was then connected and the patient was moved back to the center of the magnet.

The dynamic spin-echo sequence was a routine coronal T1 spin-echo sequence obtained during contrast infusion (500–600/20–25/2, 3-mm-thick sections, 16-cm FOV, 256 × 128 matrix, scan time of 2 minutes to 2 minutes 41 seconds). One third of a routine 0.1 mM/kg dose of gadopentetate dimeglumine was infused over 30 seconds before the start of data acquisition for the dynamic spin-echo scan sequence. After one third of the contrast material was infused, the technologist began image acquisition. The remaining two thirds of the contrast material was infused over 1 minute 30 seconds during the dynamic spin-echo sequence image acquisition. At the end of contrast infusion, a saline flush was injected to clear the tube and arm veins of contrast agent. The dynamic spin-echo scan was obtained in approximately 2 minutes 40 seconds. Immediately after the dynamic spin-echo scan was completed, without prescanning, a standard postcontrast sequence was obtained (500–600/20–25/4, 3-mm-thick sections, 16-cm FOV, 256 × 128 matrix, 5-minute 10-second scan time). Data acquisition for the standard postcontrast sequence began immediately after the dynamic spin-echo sequence, approximately 1 minute after the end of the contrast injection.

Study Population

The study population comprised the 64 patients in whom a new pituitary microadenoma or microlesion (less than 1 cm in diameter) was confidently identified. Five patients were men and 59 were women; ages ranged from 18 to 44 years (average, 35 years). The most frequent clinical reason for referral was menstrual irregularity or an abnormal hormone level. Pituitary hormone data were available in 34 patients. Twenty-six patients had an elevated prolactin level. Two patients had known Cushing syndrome and the adenomas identified in these patients were surgically removed. Several patients were referred for nonspecific problems, mainly headache. In six of these patients, pituitary hormone levels were normal. Most of the patients with hyperprolactinemia were being managed with bromocriptine at the time of the MR imaging examination.

Lesion Detection

Lesions were typically identified as a focal area of hypointensity within the pituitary gland. A patient was not included in the study unless the lesion was confidently determined to be 3 mm or greater in diameter. A narrow window display of the pituitary gland was used to improve lesion conspicuity, as has been previously suggested (8, 9). In addition, we required that two neuroradiologists identify each lesion on at least one of the enhanced sequences. Lesion size and morphologic characteristics were also noted. Focal regions of signal abnormality at the sella floor, caused by local magnetic susceptibility artifacts, were carefully identified and not included (10, 11). Three types of lesion were recognized: focal round or oval with relatively sharp margination, focal with irregular margins and borders, and focal but with indistinct or unsharp borders.

Lesion Grading

The 64 studies were independently and retrospectively reviewed by two neuroradiologists who were blinded to the

TABLE 2: Lesion grading and reader correlation

	Reader 1		Reader 2		Percentage of Agreement	95% Confidence Interval
	n	%	n	%		
Equal	10	16	15	23	.3889	.1730–.6425
Dynamic better than standard	30	47	27	42	.7813	.6003–.9072
Standard better than dynamic	11	17	8	12.5	.5833	.2767–.8483
Dynamic only	7	11	9	14	.7778	.3999–.9719
Standard only	6	9	5	8	.8333	.3588–.9958
Total	**64**	**100**	**64**	**100**		

Note.—Percentages have been rounded off.

specific clinical indications for the study. All three sequences—unenhanced, dynamic spin-echo, and standard postcontrast—were reviewed side by side for this retrospective evaluation. Each sequence was independently evaluated for whether a lesion was or was not identified. The dynamic spin-echo and standard postcontrast sequences were further graded by a subjective method for gland-lesion contrast conspicuity, lesion homogeneity, and discrimination of lesion margin. These three features were considered together because lesions often changed between sequences. In many lesions, either partial filling-in of the hypointense region was seen or partial filling-in of the peripheral margin occurred. Several lesions showed partial enhancement greater than the adjacent gland on one of the sequences. These three features were therefore considered together by each neuroradiologist in grading lesion visibility. Sequences were graded as to whether the lesion was better seen, less well seen, or equally well seen on the two sequences.

Side-by-side assessment was chosen to emphasize confidence in lesion presence and detectability. This is a significant problem in the pituitary, where surgical proof of a lesion is frequently lacking owing to long-term medical management with hormone-suppression therapy. The focus of this study was on changes in confidently recognized lesions. Side-by-side evaluation allowed sequence comparison while sacrificing blinded lesion detection statistics for any single sequence. Because of the side-by-side review, κ statistical evaluation of the data was not performed. Paired agreement statistics were used to reinforce that the trend in lesion grading was statistically consistent between the two observers.

Lesion grading established five categories of lesion visualization between the two enhanced sequences: equal, dynamic better, standard better, dynamic only, and standard only. The frequency of lesion detection within these five categories was tabulated. The percentage of paired agreement was tabulated and a 95% confidence interval was calculated for each category.

Results

Thirty-three lesions (51.5%) were focal round or focal oval in appearance with relatively sharp margins. Eighteen lesions (28%) were focal with irregular margins but with sharply defined borders. Thirteen lesions (20%) were focal but with a diffuse peripheral border. Lesion size varied from 3 mm to 10 mm (average, 5.3 mm).

Lesion grading and paired agreement results between observers are summarized in Table 2. Lesions were identified on one of the two enhanced sequences in all patients. This was a component of the inclusion criteria. In 45% to 50% of patients, the lesion, or a focal region of signal abnormality, was noted on the unenhanced sequence. These were typically regions of hypointensity. In six cases, small focal areas of hyperintensity, most likely the result of slight lesion hemorrhage, were also noted. Lesions were judged to be equally well seen on the dynamic and standard sequences in only 16% of cases by reader 1 and in 23% of cases by reader 2.

The dynamic spin-echo sequence was judged better than the standard postcontrast sequence for lesion detection in 42% to 47% of cases (Fig 1). Reduced lesion visibility on the standard postcontrast sequence was usually due to progressive lesion enhancement with diminished contrast discrimination between the lesion and the adjacent normal gland. In eight patients, reduced lesion visibility was due to a reduction in lesion size caused by a partial filling-in or enhancement of the lesion at its border (Fig 1). In eight patients, lesions became nearly isointense with the adjacent normal gland with only faint lesion detection. This was due to progressive enhancement of the lesion in six of eight patients (Fig 2) and to early reduction in enhancement of the adjacent normal gland in eight of eight patients (Fig 3).

The standard postcontrast sequence was judged better than the dynamic spin-echo se-

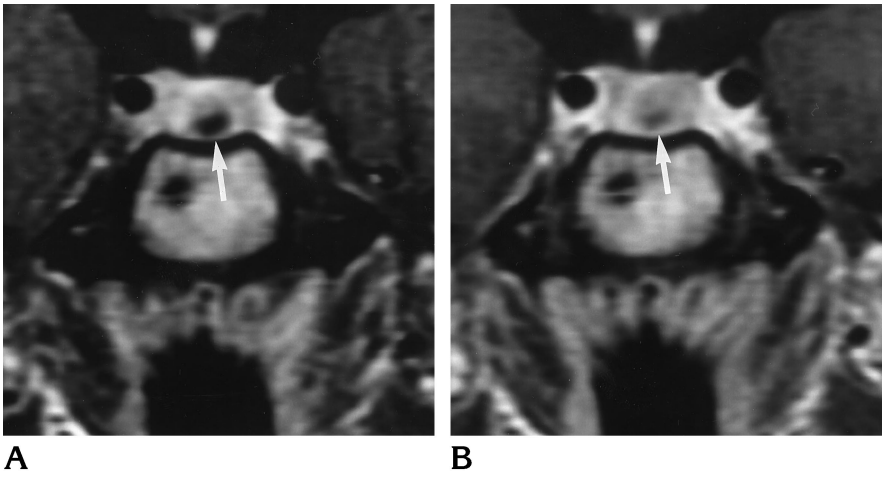

Fig 1. Near-complete filling-in of a lesion.

A, Dynamic coronal T1-weighted image (600/23/2, 16-cm FOV, 256 × 128, 3-mm-thick sections) shows a sharply marginated focal hypointense lesion (*arrow*) with an adjacent region of intermediate intensity.

B, Standard coronal T1-weighted image (600/23/4, 16-cm FOV, 256 × 128 matrix, 3-mm-thick sections) shows that significant enhancement of the lesion (*arrow*) has occurred at its periphery. The lesion appears smaller and less conspicuous than in *A*.

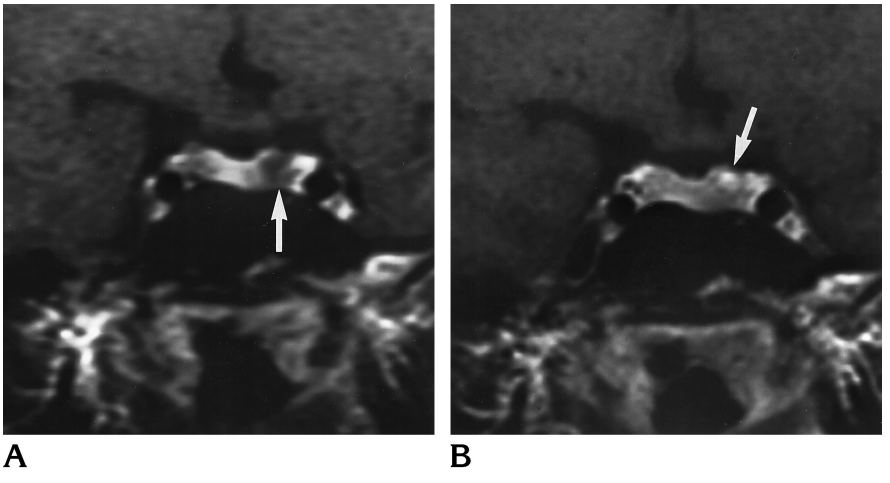

Fig 2. Progressive lesion enhancement.

A Dynamic coronal T1-weighted image (500/25/2, 16-cm FOV, 256 × 128 matrix, 3-mm-thick sections) shows an irregular focal lesion (*arrow*).

B, Standard coronal T1-weighted image (500/25/4, 16-cm FOV, 256 × 128 matrix, 3-mm-thick sections) shows that progressive enhancement of the lesion has occurred with a decrease in gland enhancement. This renders the lesion isointense with the gland, with only a small focal enhancing area (*arrow*) as the sole clue to its location.

quence in 12.5% to 17% of patients. Decreased lesion detection on the dynamic spin-echo sequence was noted in this group. Poor early gland enhancement was identified in two patients, leading to inadequate lesion discrimination. Early lesion enhancement was noted as a cause of poor detection on the dynamic spin-echo sequence in four patients (Fig 4).

Lesions were identified on only one of the two enhanced sequences in 19% to 23.5% of patients. In 8% to 9%, lesions were seen only on the standard postcontrast sequence while in 11% to 14%, lesions were identified only on the dynamic spin-echo sequence obtained during contrast administration (Fig 5).

In four patients (6%), lesions enhanced relative to the adjacent gland on the standard postcontrast enhanced sequence (Fig 2). In two patients, the lesion was seen as a focal hypointense region on the unenhanced and dynamic spin-echo sequences. In two patients, the lesion was poorly seen on the dynamic spin-echo sequence. This was due to early enhancement of the lesion and the gland, with delayed washout of contrast material from the lesion.

In six patients, the lesion identified at MR imaging was surgically removed. In all six patients, an adenoma was found and the location corresponded to the lesion identified on the MR study.

Discussion

Loss of lesion visibility has been noted on delayed MR imaging studies (12). It has been suggested that a delay in MR imaging could lead to equalization in gland-lesion contrast and reduction in adenoma detection. The temporal variation of adenoma and gland enhancement has also been documented by other authors using different MR imaging techniques (3–7). Miki et al (3) demonstrated that maximum pi-

Fig 3. Significant reduction in gland enhancement.

A, Unenhanced coronal T1-weighted image (500/25/2, 16-cm FOV, 256 × 192 matrix, 3-mm-thick sections) shows the lesion (*arrow*) to be focal and slightly hyperintense owing to hemorrhage.

B, Dynamic coronal T1-weighted image (500/25/2, 16-cm FOV, 256 × 128 matrix, 3-mm-thick sections) shows intense gland enhancement with sharp lesion definition (*arrow*).

C, Standard coronal T1-weighted image (500/25/4, 16-cm FOV, 256 × 128 matrix, 3-mm-thick sections) shows significant reduction in gland enhancement with some increase in lesion (*arrow*) signal intensity. The lesion is less conspicuous.

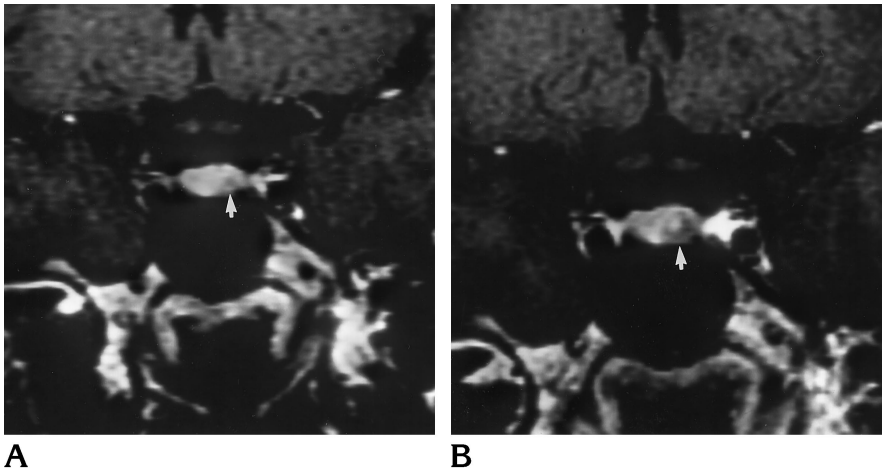

Fig 4. Better lesion visibility on standard sequence.

A, Dynamic coronal T1-weighted image (600/25/2, 16-cm FOV, 256 × 128 matrix, 3-mm-thick sections) shows a small lesion (*arrow*).

B, Standard coronal T1-weighted image (600/25/4, 16-cm FOV, 256 × 128 matrix, 3-mm-thick sections) shows more confident lesion identification with progressive reduction of gland and lesion enhancement. The lesion (*arrow*) is significantly larger than suspected on *A*.

tuitary gland enhancement typically occurred within the first 1 to 2 minutes after contrast infusion. Similar rates of gland enhancement have been described by other authors (4–7). The rate of microadenoma enhancement is less predictable. One study found that adenoma enhancement peaked at 2 to 4 minutes and that the maximum gland-lesion contrast difference occurred 1 to 3 minutes after contrast infusion (3). Sakamoto et al (4) noted that maximum lesion enhancement varied from 20 to 200 seconds after contrast infusion. A similar finding was documented in a study by Kucharczyk et al (7), in which a lesion was best seen 40 to 60 seconds after injection and was isointense with normal gland on the routine postcontrast sequence. The maximum difference in contrast between lesion and gland was typically early, in the first 3 to 4 minutes after contrast infusion. Further evidence of variation in lesion detection was presented in a CT study by Bonneville et al (13). While most adenomas in that study were typically seen as hypodense after dynamic contrast infusion, 35% of cases showed adenoma enhancement before enhancement of the pituitary portal system. This suggested that an early arterial blood supply to adenomas may be present.

Our study demonstrates that variations in lesion enhancement can be reproduced with tra-

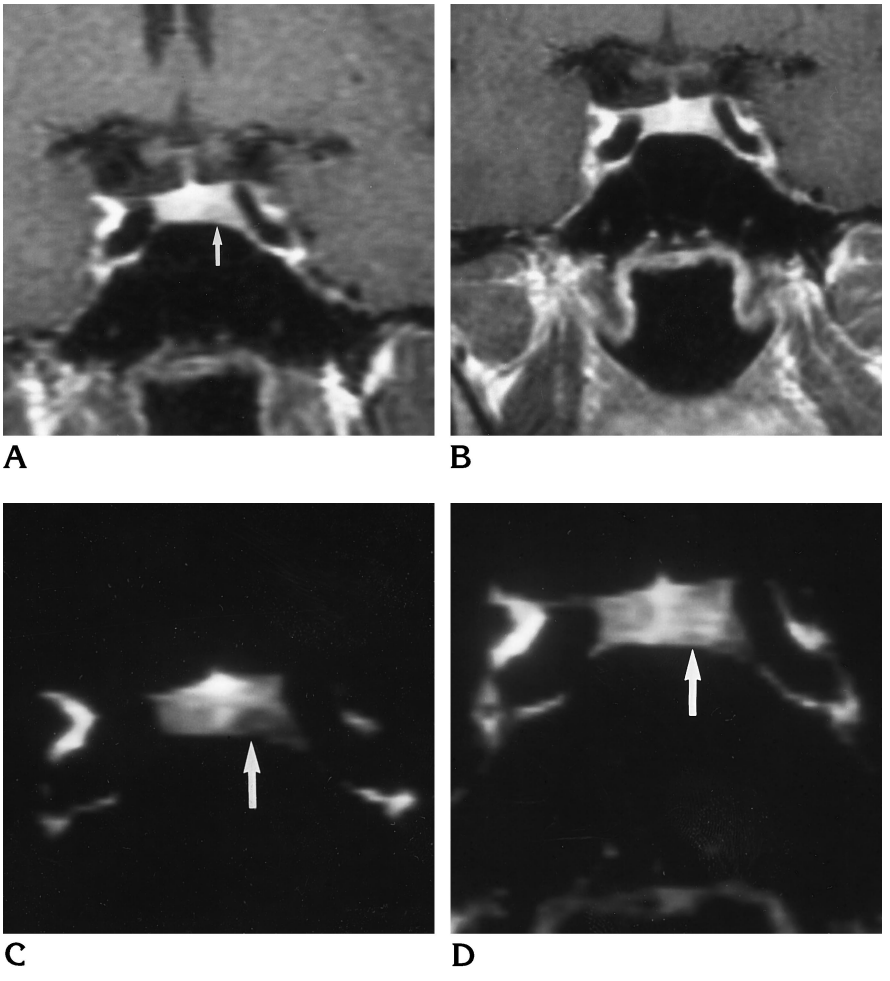

Fig 5. Lesion seen only on dynamic series.

A, Dynamic coronal T1-weighted image (500/20/2, 16-cm FOV 256 × 128 matrix, 3-mm-thick sections) shows lesion (*arrow*) on the left.

B, Standard coronal T1-weighted image (500/20/4, 16-cm FOV, 256 × 128 matrix, 3-mm-thick sections) shows normal-appearing gland.

C, Dynamic coronal T1-weighted image (500/20/2, 16-cm FOV, 256 × 128 matrix, 3-mm-thick sections) with narrow window shows a hypointense lesion (*arrow*) on the left.

D, Standard coronal T1-weighted image (500/20/4, 16-cm FOV, 256 × 128 matrix, 3-mm-thick sections) with narrow window does not show the lesion.

ditional spin-echo techniques obtained within the first few minutes during contrast infusion. In addition, improved detection and clarity of pituitary lesions was achieved by using a dynamic traditional spin-echo technique as compared with routine scanning after contrast administration. Our technique used two traditional spin-echo T1-weighted sequences: the first obtained during contrast infusion and the second after contrast administration. Standard traditional spin-echo parameters were used to take advantage of the early maximum contrast difference between gland and lesion. The dynamic traditional spin-echo sequence is essentially a standard method of pituitary evaluation using two signal averages. The sequence resulted in excellent signal-to-noise ratio and adequate gland homogeneity. This sequence was easy to perform and did not increase the study time, since it was obtained during contrast infusion.

The data in Table 2 suggest several important issues. Lesions were judged to be equally well seen in only 16% to 23% of cases. Conspicuity of lesions, therefore, differed on the two enhanced sequences in 75% to 85% of cases. It is difficult to predict whether early or late imaging will best detect a lesion in any single patient.

Imaging during infusion (early, while contrast material is reaching the gland), was the optimum technique in 53% to 61% of all cases. Lesions were seen better on the dynamic spin-echo sequence in 42% to 47% of cases and were detected only on the dynamic spin-echo scan in 11% to 14% of patients. This is consistent with previous studies, which have shown that maximum lesion-to-gland signal differences occur shortly after contrast infusion (3–7).

While the dynamic spin-echo sequence was usually better at showing lesions, the standard postcontrast sequence may still be considered a critical part of the examination. Lesions were judged to be seen better on this sequence in 12.5% to 17% of cases, and lesions were identified only on the standard postcontrast study in

8% to 9.5% of cases. While the dynamic spin-echo sequence was better at lesion detection in most instances, in a moderate number of cases (20% to 27%), the lesions were detected better on the standard postcontrast scan. Lesions were seen on only one enhanced sequence in approximately 20% of patients. This implies that lesions may be missed if either enhanced sequence is eliminated.

The results of our study are not surprising. Variation in lesion detection is an expected consequence of the rate of time-dependent enhancement of two structures (such as gland versus lesion) over time. Our results reinforce the findings of previous studies, which have shown that gland and lesion contrast enhancement change rapidly in the first 5 minutes after contrast infusion (3–7). The rate of gland and lesion enhancement is unpredictable. Imaging at two points in time optimizes lesion detection.

Lesion enhancement relative to adjacent gland was identified in four (6%) of our patients. Two of these lesions that enhanced relative to the gland on the standard postcontrast sequence were seen on the dynamic spin-echo sequence. This was most likely due to early enhancement of the lesion with a similar gland-to-lesion signal intensity. Early lesion enhancement, before pituitary portal enhancement, was described by Bonneville et al (13), who used a dynamic CT technique. Several reports have evaluated the time course of hypothalamic pituitary portal flow, and early microadenoma enhancement by the arterial blood supply has been suggested. In two other of our patients, while enhancement of the lesion was seen on the standard postcontrast sequence, the lesion was hypointense and clearly identified on the dynamic spin-echo sequence. This was most likely due to slower lesion enhancement with progressive washout of contrast within the normal gland and delayed washout of contrast from the lesion. Previous authors have noted this "flip-flop" effect (14–16).

The injection technique used in our study was designed to accomplish two goals: to obtain a sequence during maximum gland-to-lesion enhancement differences and to obtain a routine postcontrast sequence at a set time after contrast infusion. Administering the bolus over the first two thirds of the dynamic sequence was chosen to create uniform delivery during early scanning. The recommended slow rate of contrast infusion was one of the factors that initiated the use of our dynamic approach. The timing of the standard postcontrast sequence was similar to a routine enhanced sequence obtained after contrast infusion when one factors in patient repositioning and sequence prescanning.

Side-by-side assessment of lesions was chosen to emphasize changes in confidently detected lesions. This is a significant problem in pituitary studies, in which surgical proof of a lesion is frequently lacking owing to long-term medical management with hormone-suppression therapy. Side-by-side evaluation allowed sequence comparison while sacrificing blinded lesion detection statistics for any single sequence. In spite of the side-by-side review, 19% to 23.5% of confidently identified lesions were not visible on one of the two enhanced sequences even when lesion location was provided by the other two sequences. This reinforces the idea that lesions can become invisible on any single enhanced sequence.

Imaging sequences were graded for three specific characteristics: contrast conspicuity between the lesion and adjacent normal gland, homogeneity of the hypointense lesion, and crispness or clarity of the lesion margin. Measurement of signal differences between the lesion and the adjacent normal gland was not used in our study. This approach is justified for several reasons. We observed that lesions frequently changed between sequences. Alteration in gland signal intensity was often seen with progressive enhancement or filling-in of the hypointense lesion. Many lesions were nonhomogeneous on one or both sequences, and an average region of interest would not, in these instances, truly reflect lesion conspicuity. In addition, lesion enhancement was seen on one sequence, with several lesions developing higher signal relative to gland. Our subjective assessment allowed all of these characteristics to be included into a simple grading system: equal, better, or reduced lesion visibility.

The time variation in lesion visibility after contrast injection is a factor to consider when comparing any two techniques for evaluation of pituitary lesions. The difference in lesions detected with the dynamic traditional spin-echo technique in our study will most likely occur when any two sequences are compared after contrast enhancement of the pituitary gland. The choice of which technique to perform first could have a dramatic impact on lesion detec-

tion and/or on the statistical results of technique comparison after contrast administration.

Some investigators have suggested that a reduced dose of MR imaging contrast is equivalent to a standard dose of contrast for microadenoma detection (17, 18). Because data acquisition for a standard enhanced sequence typically begins after realignment of the patient in the magnet and prescanning has occurred, image acquisition is likely to begin at the point of maximum gland enhancement, and most data are obtained during the washout of contrast from both lesion and gland. In one study, normalized infundibular and posterior pituitary signal were actually lower on the full-dose sequence than on the half-dose sequence (18).

This report focuses on our experience with the dynamic traditional spin-echo technique at 1.5 T. We have had less favorable results with this technique on a 0.5-T system, in which the dynamic spin-echo sequence (with 3-mm-thick sections, 15- to 20-cm FOV, and two data averages) tends to have poor signal.

In conclusion, dynamic traditional spin-echo imaging of the pituitary gland provides improved visibility and clarity of lesions as compared with only routine scanning after contrast administration. Our dynamic technique was easy to perform and did not add a time penalty to the pituitary study. The practice of examining the gland twice, once during and once after contrast infusion, was effective.

Acknowledgments

We thank Richard Day for his assistance with statistical analysis and Dawn Scheib for her assistance with manuscript preparation.

References

1. Hemminghytt S, Kalkhoff RK, Daniels DL, Williams AL, Grogan JP, Haughton VM. Computed tomographic study of hormone-secreting microadenomas. *Radiology* 1983;46:65–69
2. Bonneville JF, Cattin F, Moussa-Bacha K, Portha C. Dynamic computed tomography of the pituitary gland: the "tuft sign." *Radiology* 1983;149:145–148
3. Miki Y, Michimasa M, Nishizawa S, et al. Pituitary adenomas and normal pituitary tissue: enhancement patterns on gadopentetate-enhanced MR imaging. *Radiology* 1990;177:35–38
4. Sakamoto Y, Takahashi M, Korogi Y, Bussaka H, Ushio Y. Normal and abnormal pituitary glands: gadopentetate dimeglumine-enhanced MR imaging. *Radiology* 1991;178:441–445
5. Finelli DA, Kaufman B. Varied microcirculation of pituitary adenomas at rapid, dynamic, contrast-enhanced MR imaging. *Radiology* 1993;189:205–210
6. Yuh WTC, Fisher DJ, Nguyen HD, et al. Sequential MR enhancement pattern in normal pituitary gland and in pituitary adenoma. *AJNR Am J Neuroradiol* 1994;15:101–108
7. Kucharczyk W, Bishop JE, Plewers DB, Keller MA, George S. Detection of pituitary microadenomas: comparison of dynamic keyhole fast spin-echo, unenhanced and conventional contrast-enhanced MR imaging. *AJR Am J Roentgenol* 1994;163:671–679
8. Kucharczyk W, Davis DO, Kelly WM, Sze G, Norman D, Newton TH. Pituitary adenomas: high resolution MR imaging at 1.5T. *Radiology* 1986;161:761–765
9. Kulkarni MV, Lee KF, McArdle CB, Yeakley JW, Haar FL. 1.5-T MR imaging of pituitary microadenomas: technical considerations and CT correlation. *AJNR Am J Neuroradiol* 1988;9:5–11
10. Sakurai K, Fujita N, Harada K, Kim SW, Nakanishi K, Kozuka T. Magnetic susceptibility artifact in spin-echo MR imaging of the pituitary gland. *AJNR Am J Neuroradiol* 1993;13:1301–1308
11. Elster AD. Sellar susceptibility artifacts: theory and implications. *AJNR Am J Neuroradiol* 1993;14:129–136
12. Davis PC, Hoffman JC, Malko JA, et al. Gadolinium-DTPA and MR imaging of pituitary adenoma: a preliminary report. *AJNR Am J Neuroradiol* 1987;8:817–823
13. Bonneville JF, Cattin F, Gorczyca W, Hardy J. Pituitary microadenomas: early enhancement with dynamic CT–implications of arterial blood supply and potential importance. *Radiology* 1993; 187:857–861
14. Dwyer AJ, Frank JA, Doppman JL, et al. Pituitary adenomas in patients with Cushing disease: initial experience with Gd-DTPA-enhanced MR imaging. *Radiology* 1987;163:421–426
15. Doppman JL, Frank JA, Dwyer AJ, et al. Gadolinium DTPA enhanced MR imaging of ACTH-secreting microadenomas of the pituitary gland. *J Comput Assist Tomogr* 1988;12:728–735
16. Newton DR, Dillon WP, Norman D, Newton TH, Wilson CB. Gd-DTPA-enhanced imaging of pituitary adenomas. *AJNR Am J Neuroradiol* 1989;10:949–954
17. Davis PC, Gokhale KA, Joseph GJ, et al. Pituitary adenoma: correlation of half-dose gadolinium-enhanced MR imaging with surgical findings in 26 patients. *Radiology* 1991;180:779–784
18. Giacometti AR, Joseph GJ, Peterson JE, Davis PC. Comparison of full- and half-dose gadolinium-DTPA: MR imaging of the normal sella. *AJNR Am J Neuroradiol* 1993;14:123–127